British Journal of Pharmacology (1999) 128, 1291–1299
http://www.stockton-press.co.uk/bjp

Pharmacological similarities between native brain and heterologously expressed α4β2 nicotinic receptors

[1]Navid Shafaee, [1]McCann Houng, [1]Anthony Truong, [1]Nareerat Viseshakul, [1]Antonio Figl, [2]Sumandeep Sandhu, [3]John R. Forsayeth, [4]Linda P. Dwoskin, [4]Peter A. Crooks & *,[1]Bruce N. Cohen

[1]Division of Biomedical Sciences, University of California, Riverside, California, CA 92521-0121, U.S.A. [2]Department of Environmental Toxicology, University of California, Riverside, California, CA 92521-0121, U.S.A.; [3]Elan Pharmaceuticals, 3760 Haven Ave., Menlo Park, CA 94025-1012, U.S.A. and [4]Pharmacology & Experimental Therapeutics, College of Pharmacy, University of Kentucky, Lexington, Kentucky, KY 40536-0082, U.S.A.

1 We studied the pharmacological properties of native rat brain and heterologously expressed rat α4β2 nicotinic receptors immunoprecipitated onto a fixed substrate with the anti-α4 antibody mAb 299.

2 Immunodepletion with the anti-β2 antibody mAb 270 showed that 89% of the mAb-299-precipitated rat brain receptors contained β2.

3 The association and dissociation rate constants for 30 pM ±[^{3}H]-epibatidine binding to α4β2 receptors expressed in oocytes were 0.02±0.01 and 0.03±0.01 min^{-1} (±standard error, degrees of freedom = 7–8) at 20–23°C.

4 The Hill coefficients for ±[^{3}H]epibatidine binding to the native brain, α4β2 receptors expressed in oocytes, and α4β2 receptors expressed in CV-1 cells (using recombinant adenovirus) were 0.69–0.70 suggesting a heterogeneous receptor population. Fits of the ±[^{3}H]-epibatidine concentration-binding data to a two-site model gave K_D s of 8–30 and 560–1,200 pM. The high-affinity sites comprised 73–74% of the native brain and oocyte α4β2 receptor population, 85% of the CV-1 α4β2 receptor population.

5 The expression of rat α4β2 receptors in CV-1 cells using vaccinia viral infection-transfection resulted in a more homogeneous receptor population (Hill coefficient of 1.0±0.2). Fits of the ±[^{3}H]-epibatidine binding data to a single-site model gave a K_D of 40±3 pM.

6 DHβE (IC_{50} = 260–470 nM) and the novel nicotine analogue NDNI (IC_{50} = 7–10 μM) inhibited 30 pM ±[^{3}H]-epibatidine binding to the native brain and heterologously expressed α4β2 receptors equally well.

7 The results show that α4β2-containing nicotinic receptors in the rat brain and heterologously expressed rat α4β2 receptors have similar affinities for ±[^{3}H]-epibatidine, DHβE, and NDNI.

Keywords: Neuronal nicotinic acetylcholine receptors; α4; β2; *Xenopus* oocytes; dihydro-β-erythroidine; epibatidine binding; immunoprecipitation; mAb 299 antibody

Abbreviations: ACh, acetylcholine; AV, adenoviral expression; df, degrees of freedom; CMV, cytomegaloviral; DHβE, dihydro-β-erythroidine; DMPP, dimethylphenylpiperazinium; NDNI, N-n-decylnicotinium iodide; n_H, apparent Hill coefficient; SCG, superior cervical ganglion; SCID, severe combined immunodeficient; s.e., standard error; s.e.m., standard error of the mean; VV, vaccinia viral infection-transfection

Introduction

Several lines of evidence suggest that the predominant mammalian brain nicotinic subtype contains α4 and β2 subunits. First, the α4 and β2 mRNAs are the most abundant and widespread nicotinic subunit mRNAs in the rat brain (Zoli *et al*., 1995). Second, the α4 subunit forms functional nicotinic receptors with the β2 subunit in heterologous expression systems (reviewed in Sargent, 1993). Third, the α4 and β2 subunits co-assemble into a brain nicotinic receptor (Whiting & Lindstrom, 1987) that accounts for most of the high-affinity rat brain [^{3}H]-cytisine binding (Flores *et al*., 1991). Fourth, immunohistochemical localization confirms the widespread distribution of the β2 protein in the rat brain (Hill *et al*., 1993) and immunodepletion with the anti-β2 antibody mAb 270 removes 92% of the [^{3}H]-nicotine binding sites from rat brain extracts (Whiting & Lindstrom, 1986). Fifth and finally, knocking out the β2 gene eliminates virtually all the high-affinity mouse brain [^{3}H]-nicotine binding sites and most of the high-affinity ±[^{3}H]-epibatidine binding sites (Picciotto *et al*., 1995; Zoli *et al*., 1998). Similarly, knocking out the α4 gene also removes most of these binding sites (Marubio *et al*., 1999).

Nevertheless, rat forebrain homogenates appear to contain at least two major classes of ±[^{3}H]-epibatidine binding sites (Houghtling *et al*., 1995). The K_Ds for ±[^{3}H]-epibatidine binding to the high- and low-affinity sites are 15±4 pM (mean±standard error (s.e.)) and 360±150 pM at 24°C (Houghtling *et al*., 1995). Both sites display characteristic neuronal nicotinic pharmacological profiles. The similarity between the high-affinity rat brain K_D and the K_D for ±[^{3}H]-epibatidine binding to chick α4β2 receptors expressed in M10 cells (4.1±0.3 pM at 24°C) suggests that the high-affinity rat brain sites are α4β2 receptors (Houghtling *et al*., 1995). The subunit composition of the low-affinity binding site in the rat brain is unclear. The differences between ±[^{3}H]-epibatidine binding to the rat brain receptors and the chick α4β2 receptors expressed in M10 cells are not due to methodological differences because the assay conditions for both receptors were identical (Houghtling *et al*., 1995).

*Author for correspondence; E-mail: jsei@citrus.ucr.edu

Mouse brain synaptosomes also appear to contain two major classes of nicotinic receptors that mediate α-bungarotoxin insensitive ACh-induced $^{86}Rb^+$ efflux (Marks *et al*., 1999). The EC_{50}s of these two receptor classes for ACh-induced $^{86}Rb^+$ efflux are 7.2 ± 0.3 μM ACh (mean ± standard error of the mean s.e.m.) and 550 ± 60 μM ACh (Marks *et al*., 1999). The nicotinic antagonist dihydro-β-erythroidine (DHβE) inhibits $^{86}Rb^+$ efflux through the more ACh-sensitive receptors ~ten times more potently (IC_{50} of 0.2 μM DHβE) than it inhibits $^{86}Rb^+$ efflux through the less ACh-sensitive receptors (IC_{50} of 3 μM DHβE) (Marks *et al*., 1999). Both receptor types are distributed throughout the brain and contain β2 nicotinic subunits (Marks *et al*., 1999). A regional correlation between high-affinity nicotine binding and DHβE-sensitive $^{86}Rb^+$ efflux in the brain suggests that the DHβE-sensitive receptors are α4β2 nicotinic receptors (Marks *et al*., 1999). However, the identity of the DHβE-insensitive receptors is unclear.

±[^{3}H]-Epibatidine binding to immunoprecipitated receptors allows us to compare the pharmacological properties of isolated native brain nicotinic receptors containing a known subunit with those of heterologously expressed nicotinic receptor subtypes, under identical experimental conditions and without confounding intracellular factors. To determine whether α4-containing rat brain nicotinic receptors and heterologously expressed rat α4β2 nicotinic receptors exhibit both high- and low-affinity ±[^{3}H]-epibatidine binding, we immunoprecipitated solubilized nicotinic receptors with the anti-α4 antibody mAb 299 (Whiting & Lindstrom, 1988) and measured their ±[^{3}H]-epibatidine concentration-binding reactions. The results show that both receptor types display high- and low-affinity ±[^{3}H]-epibatidine binding. To determine whether the antagonist profile of the high-affinity native receptors matched that of the high-affinity heterologously expressed receptors, we measured the ability of two competitive antagonists (DHβE, N-n-decylnicotinium iodide (NDNI)) to inhibit 30 pM ±[^{3}H]-epibatidine binding to these receptors. Previous studies show that DHβE inhibits high-affinity ±[^{3}H]-epibatidine binding to rat forebrain homogenates (Houghtling *et al*., 1995). NDNI is a novel nicotine analogue. The results show that the high-affinity native brain and heterologously expressed α4β2 receptors exhibit similar K_is for DHβE and NDNI.

Methods

Solubilization of rat brain receptors

Adult rats were killed by an overdose of pentobarbital sodium or CO_2 inhalation according to the guidelines of the University of California Animal Use Committee. After killing the rats, the entire brain was removed and frozen immediately in liquid nitrogen. Homogenates were prepared from the frozen brains using a previous protocol (Gerzanich *et al*., 1995). The brain homogenates were stored at −80°C in a lysis buffer containing (mM): NaCl 50, Na phosphate buffer 50, EGTA 5, EDTA 5, 2% Triton X-100, and Complete™ protease inhibitor (1 tablet per 40 ml of lysis buffer, Boehringer Mannheim, Indianapolis, IN, U.S.A.). We used a $CuSO_4$ assay (Micro BCA Protein Assay, Pierce, Rockford, IL, U.S.A.) to measure the homogenate total protein concentration.

Oocyte expression

Stage V–VI oocytes were surgically isolated from anaesthetized *Xenopus* using a previous protocol (Quick & Lester, 1994) in accordance with the guidelines of the University of California Animal Use Committee. Capped rat α4-1 and β2 cRNAs were synthesized *in vitro* from linearized pBluescript plasmids using the mMessage mMachine RNA transcription kit (Ambion, Austin, TX, U.S.A.). The most probable subunit stoichiometry for α4β2 receptors expressed in *Xenopus* oocytes is $(\alpha4)_2(\beta2)_3$ (Cooper *et al*., 1991). Therefore, we injected the α4 and β2 cRNAs in a 2 : 3 (weight/weight) stoichiometric ratio. Each oocyte received 15 ng of α4-1 RNA and 22.5 ng of β2 RNA. The injected oocytes were incubated for 2–3 days in a modified Barth's solution (mM): NaCl 96, HEPES 5, Na-pyruvate 2.5, KCl 2, $CaCl_2$ 1.8, $MgCl_2$ 1, 2.5 μg ml^{-1} gentamycin, 5% horse serum, pH 7.4 at 18°C. The oocytes were then solubilized as previously described (Peng *et al*., 1994; Gerzanich *et al*., 1995) using the same buffer that we used for the rat brain receptors (see above).

Adenoviral expression in CV-1 cells

Recombinant adenoviruses encoding the rat nicotinic α4 subunit (Adtetα4), the rat nicotinic β2 subunit (Adtetβ2), and the tetracycline-dependent trans-activator (AdtTA) were prepared as described previously (Neering *et al*., 1996; Hardy *et al*., 1997) using a tetracycline-regulated promoter (Gossen & Bujard, 1992), rather than a simple CMV one. Recombinant adenoviruses were purified from infected HEK cells using a CsCl gradient (Jones & Shenk, 1979). The virus titer was determined from the OD_{260} (1 OD unit = 5×10^{10} plaque-forming units (p.f.u.) in HeLa cells). Ten p.f.u. of each virus (Adtetα4, Adtetβ2, AdtTA) were added per cell to a just confluent CV-1 monolayer to express the α4β2 receptors. After a 24 h incubation, the cells were washed with PBS, frozen at −80°C, and then thawed in the lysis buffer (above). After thawing and lysis, the homogenate was centrifuged at 13,000 r.p.m. The supernatant was removed and frozen at −80°C.

Vaccinia viral expression in CV-1 cells

The rat α4 and β2 subunits cDNAs were excised from pBluescript and subcloned into the vaccinia expression vector pTM1 (Elroy-Stein *et al*., 1989) to obtain the cDNA plasmids pTM1α4 and pTM1β2. Expression in pTM1 is under the control of a T7 RNA polymerase promoter, aided by cap-independent translation conferred by the encephalomyocarditis virus 5′ untranslated leader sequence (Elroy-Stein *et al*., 1989). CV-1 cells, grown to 60–70% confluence in 83 cm^2 flasks in a 5% CO_2 incubator, were infected with the recombinant vaccinia virus VTF7-3 (Fuerst *et al*., 1986). The cells were infected at a multiplicity of infection of five viral particles per cell for 30 min at 37°C in serum-free MEM medium supplemented with non-essential amino acids and sodium pyruvate. VTF7-3 is a recombinant virus that continuously expresses T7 RNA polymerase in infected cells. After infection, CV-1 cells were washed three times in MEM medium and each flask was transfected with 4 μg of pTM1α4, 4 μg of pTM1β2, and 24 μl lipofectin in serum-free MEM medium. The DNA-lipofectin mixture was allowed to adsorb to the cells for 16 h at 37°C. After this incubation, the CV-1 cells were washed three times and allowed to recover in MEM medium supplemented with 0.1 mM non-essential amino acids, 1 mM sodium pyruvate, streptomycin (100 mg ml^{-1}), and penicillin (100 units ml^{-1}). After recovery, the infected-transfected cells were frozen at −80°C prior to solubilization in the same buffer used for the oocyte and rat brain experiments.

Measurement of ±[^{3}H]-epibatidine binding

±[^{3}H]-epibatidine (specific activity 50–60 Cimmol^{-1}) was purchased from Amersham Life Science, Inc. (Arlington Heights, IL, U.S.A.). We followed previous protocols (Peng *et al*., 1994; Gerzanich *et al*., 1995) to measure ±[^{3}H]-epibatidine binding to the immunoprecipitated receptors. The wells of EIA/RIA strip plates (Costar Corning Corp., Cambridge, MA, U.S.A.) were coated with purified mAb 299 (Research Biochemicals, Natick, MA, U.S.A.) by adding 0.5 or 2 μg of mAb 299 in 100 μl of 10 mM Na bicarbonate (pH 8.8) for an overnight incubation at 4°C. We blocked the coated wells with 3% bovine serum albumin in 200 μl of PBS-Tween buffer (100 mM NaCl, 10 mM Na phosphate, 0.05% Tween 20, pH 7.5) for 2 h at 4°C and rinsed the blocked wells three times with PBS-Tween buffer. Aliquot parts (100 μl) of the solubilized receptors in lysis buffer were added to the wells and incubated overnight at 4°C. We rinsed the wells three times with PBS-Tween the following day and added the appropriate ±[^{3}H]-epibatidine concentration in PBS-Tween to each well for 4 h at 20–23°C (Houghtling *et al*., 1995). To avoid ligand depletion at low ±[^{3}H]-epibatidine concentrations (0.001–0.3 nM), we incubated each well in 2–4 ml of the ±[^{3}H]-epibatidine solution (Houghtling *et al*., 1995). At higher ±[^{3}H]-epibatidine concentrations (⩾1 nM), we used an incubation volume of 200 μl. The amount of receptor added to the wells was adjusted so that the depletion of free ±[^{3}H]-epibatidine was <10%. The free ligand concentrations in the ±[^{3}H]-epibatidine concentration-binding experiments were corrected for ligand depletion. After the ±[^{3}H]-epibatidine incubation, the wells were rinsed three times with ice-cold PBS-Tween buffer, placed whole into 1 ml of scintillation fluid, and counted. We measured nonspecific ±[^{3}H]-epibatidine binding three different ways. The first method was to measure ±[^{3}H]-epibatidine binding as described above but in the presence of 100 μM cold (−) nicotine (Houghtling *et al*., 1995). The second method (used only with the recombinant receptors) was to measure ±[^{3}H]-epibatidine binding to the immunoprecipitated protein from un-injected oocytes or uninfected CV-1 cells. The third method was to measure ±[^{3}H]-epibatidine binding to uncoated, but blocked, wells (Peng *et al*., 1994). The nonspecific binding measured by these three methods was not significantly different. Thus, ±[^{3}H]-epibatidine binding to the uncoated, blocked wells and background radiation were the main sources of nonspecific binding. The ±[^{3}H]-epibatidine concentration-binding experiments were replicated twice.

Kinetic measurements

The forward rate constant for ±[^{3}H]-epibatidine binding to the α4β2 receptors expressed in oocytes at 20–23°C was measured by placing wells containing the immunoprecipitated receptors in 4 ml of 0.03 nM ±[^{3}H]-epibatidine for times ranging from 1–300 min. The forward binding reaction was stopped by adding an excess (1 mM) of cold (−)-nicotine. After stopping the reaction, we rinsed the wells three times with ice-cold PBS-Tween and counted the bound ±[^{3}H]-epibatidine. The backward rate constant for ±[^{3}H]-epibatidine binding to the α4β2 receptors at 20–23°C was measured by incubating wells containing the immunoprecipitated receptors in 4 ml of 0.03 mM ±[^{3}H]-epibatidine for 4 h. After the 4 h incubation, we stopped the reaction by adding 1 mM cold (−)-nicotine to the wells. At times ranging from 1–600 min after adding the nicotine, the wells were rinsed three times with ice-cold PBS-Tween and counted. Nonspecific binding was measured by adding 1 mM cold (−)-nicotine to the 0.03 nM ±[^{3}H]-epibatidine incubations.

Inhibition of ±[^{3}H]-epibatidine binding

NDNI was synthesized according to the method of Crooks *et al*. (1995). The IC_{50} of DHβE and NDNI for inhibiting ±[^{3}H]-epibatidine binding was estimated by fitting the inhibitor concentration-binding data to the following equation:

$$B = \frac{B_{max}}{1 + \left(\frac{[I]}{IC_{50}}\right)} \quad (1)$$

where [I] was the inhibitor concentration, B was the amount of bound ±[^{3}H]-epibatidine, and B_{max} was the maximum bound ±[^{3}H]-epibatidine. The errors reported for the fitted parameters (n_H, K_D, IC_{50}, B_{max}, k_f, k_b, etc.) are s.e.s. The degrees of freedom (d.f.) associated with these errors are the number of points in the graph (number of different concentration or time measurements) minus two. The K_i for inhibition was calculated from the following equation,

$$K_i = \frac{IC_{50}}{1 + \frac{0.03\ nM}{K_D}} \quad (2)$$

where 0.03 nM was the ±[^{3}H]-epibatidine concentration used to measure the IC_{50}. To calculate the s.e. for the K_i, we used the following approximation,

$$K_i \approx \frac{IC_{50} K_D}{0.03\ nM}. \quad (3)$$

This approximation assumes that 0.03 nM was $>>$ the K_D for the high-affinity ±[^{3}H]-epibatidine binding sites. We calculated the variance of the product ($K_D IC_{50}$) using a previously derived formula for the variance of the product of two independent random variables (Mood *et al*., 1974). To avoid radioligand depletion, the maximum number of counts bound per well in the inhibitor experiments was kept to 300–500 c.p.m. This level of binding yielded an adequate signal : noise ratio because the maximum number of counts bound per well was still 7–15 times larger than the typical amount of nonspecific binding. The inhibitor experiments were replicated 2–4 times.

Immunodepletion with mAb 270

Dr Kenneth Dorshkind (University of California, Los Angeles, CA, U.S.A.) provided the mAb 270 ascites used for the immunodepletion experiments. Further antibody purification was unnecessary because the ascites was obtained from severe combined immunodeficient (SCID) mice. Comparisons between the amount of receptor bound to wells coated with 2 μg of mAb 299 and wells coated with 2 μl of mAb 270 ascites suggest that the mAb 270 ascites contained 1–2 mg antibody ml^{-1} (assuming similar immunoprecipitation efficiencies for both antibodies). To immunodeplete the β2-containing nicotinic receptors, the rat brain extracts were subjected to three serial overnight incubations with mAb 270 at 4°C (25–50 μg antibody (μl of rat brain extract added)$^{-1}$) before immunoprecipitation onto the EIA/RIA strip plates. After each overnight incubation, 100 μl of extract was rotated with 50 μl of a 20% slurry of Protein G sepharose beads (Pharmacia, Piscataway, NJ, U.S.A.) for 3 h at 4°C to collect the immune complexes. The sample was centrifuged and the supernatant was collected after incubation with the beads. After the third mAb 270 pre-incubation, we immunoprecipi-

tated the remaining receptors onto EIA/RIA strip plates and measured ±[^{3}H]-epibatidine binding. To control for nonspecific protein loss, aliquot parts of the rat brain extract were processed exactly as above but without mAb 270.

Serial Triton X-100 extraction

To determine whether a single detergent extraction removed all of the Triton X-100-soluble nicotinic receptors from the rat brain homogenates, we performed two extractions in series. In the first extraction, rat brain tissue was solubilized with 2% Triton X-100 and centrifuged as described above. We then measured 30 nM ±[^{3}H]-epibatidine binding to the initial supernatant, re-solubilized the initial pellet in lysis buffer, centrifuged the mixture, and measured ±[^{3}H]-epibatidine binding to the supernatant from the re-solubilized pellet. The supernatant from the re-solubilized pellet contained 11% of the total ±[^{3}H]-epibatidine bound to the combined extracts from the initial homogenate and re-solubilized pellet. Therefore, a single detergent extraction removed 89% of the Triton X-100-soluble receptors from the homogenates.

MAb 299 immunoprecipitation efficiency

We used serial immunodepletions to measure the efficiency of mAb 299 immunoprecipitation. The Triton X-100 extract from oocytes expressing $\alpha4\beta2$ receptors was divided into seven groups of aliquot parts (four aliquot parts per group). Group 1 was incubated once overnight in mAb-299-coated EIA/RIA strip plate wells (2 μg antibody per well) and then the ±[^{3}H]-epibatidine bound to the wells, after a 40 min incubation in a saturating concentration of ±[^{3}H]-epibatidine (30 nM), was measured. The six remaining groups were divided into experimentals (groups 2–4 and controls (groups 5–7). Groups 2–4 were pre-incubated 1–3 times in mAb-299-coated wells before a final overnight incubation in mAb-299-coated wells. Groups 5–7 were similarly pre-incubated 1–3 times in blocked, uncoated wells before a final overnight incubation in mAb-299-coated wells. Nonspecific receptor loss was estimated by dividing ±[^{3}H]-epibatidine bound by groups 5–7 by that bound by group 1. To correct for nonspecific loss, we divided the ±[^{3}H]-epibatidine bound by the experimental groups (2–4) by the fraction of ±[^{3}H]-epibatidine binding in group 1 remaining in the corresponding control groups (5–7). Three serial pre-incubations in the mAb-299-coated wells removed >80% of the ±[^{3}H]-epibatidine binding activity from the extracts (Figure 1A, mAb 299 Immunodepleted). Three serial pre-incubations in blocked, uncoated wells removed ~20% of the ±[^{3}H]-epibatidine binding activity from the extracts (Figure 1A, Control). After correcting for nonspecific receptor loss, the amount of ±[^{3}H]-epibatidine bound to the mAb-299-precipitated receptors declined exponentially as a function of the number of mAb 299 pre-incubations (Figure 1B). Each pre-incubation removed 26% of the ±[^{3}H]-epibatidine binding activity. Thus, the mAb 299 immunoprecipitation efficiency under our experimental conditions was 26%.

Results

Kinetics of ±[^{3}H]-epibatidine binding to $\alpha4\beta2$ receptors

±[^{3}H]-Epibatidine association to (Figure 2A) and dissociation from (Figure 2B) $\alpha4\beta2$ receptors expressed in *Xenopus* oocytes followed a single-exponential time course. We used a concentration of 30 pM ±[^{3}H]-epibatidine for these experiments because our preliminary experiments suggested that it should produce 40–50% receptor occupancy. The association rate constant (k_f) for 30 pM ±[^{3}H]-epibatidine was 0.02 ± 0.01 min^{-1} (±s.e., d.f.=7) at 20–23°C. The dissociation rate constant (k_b) for the same ±[^{3}H]-epibatidine concentration was 0.03 ± 0.01 min^{-1} (d.f.=8). The receptor occupancy is given by $k_f(k_f+k_b)^{-1}$. Therefore, the kinetic data predict that 30 pM ±[^{3}H]-epibatidine should produce 40% receptor occupancy.

±[^{3}H]-Epibatidine binding to mAb-299-precipitated native brain receptors

To measure the ±[^{3}H]-epibatidine-concentration binding relation of the mAb-299-precipitated rat brain receptors, we incubated the immunoprecipitated receptors in 0.001–30 nM ±[^{3}H]-epibatidine for 4 h at 20–23°C (Figure 3). This incubation time was ~eight times longer than the $\alpha4\beta2$ ±[^{3}H]-epibatidine dissociation time constant (33 min). Similar to that ($n_H=0.73\pm0.03$) previously reported for ±[^{3}H]-epibatidine binding to rat forebrain homogenates

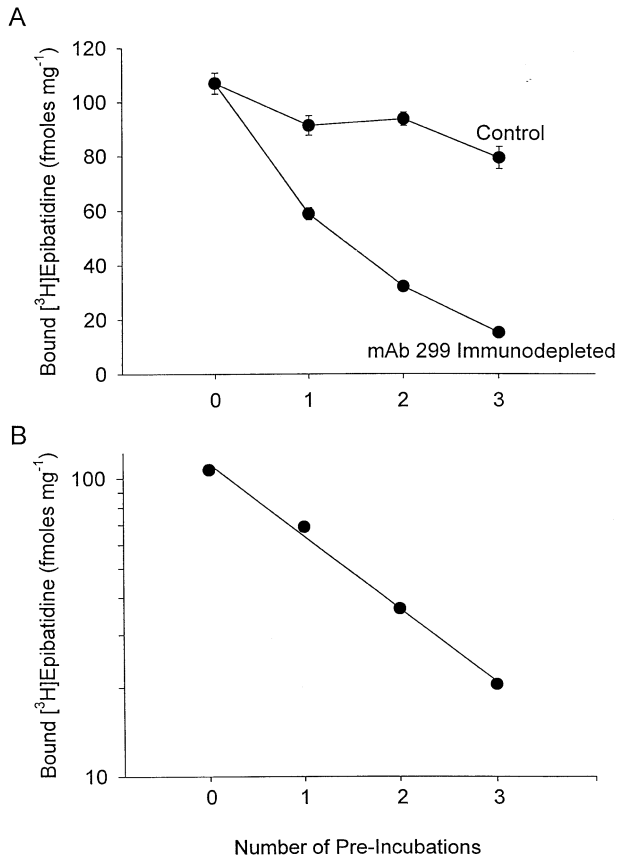

Figure 1 A single incubation in a mAb-299-coated EIA/RIA well immunoprecipitated 26% of the mAb-299-precipitable receptors in the oocyte extract. (A) The amount of ±[^{3}H]-epibatidine bound to the mAb-299-coated wells after 0–3 pre-incubations in uncoated, blocked wells (Control) or an equal number of pre-incubations in mAb-299-coated wells (mAb 299 immunodepleted). Free ±[^{3}H]-epibatidine concentration was 30 nM. See Methods for further details. Error bars are ±s.e.mean ($n=4$ replicates). (B) Semilog plot of the ±[^{3}H]-epibatidine bound to the mAb-299-coated wells after 0–3 pre-incubations mAb-299-coated wells. The bound ±[^{3}H]-epibatidine was corrected for nonspecific receptor loss. The slope of the regression line is 0.26.

(Houghtling *et al*., 1995), the Hill coefficient (0.69±0.05, d.f.=6) for ±[^{3}H]-epibatidine binding to the mAb-299-precipitated native brain receptors was less than unity, suggesting receptor heterogeneity. Therefore, we fit the ±[^{3}H]-epibatidine concentration-binding data to a two independent binding site model (Figure 3). The resulting K_Ds (11±4 pM; 560±70 pM, d.f.=8) were close to those (15±4 pM, 360±150 pM) reported previously for ±[^{3}H]-epibatidine binding to rat forebrain homogenates (Houghtling *et al*., 1995). The high-affinity site (B_{max1}=32±4 fmol (mg protein)$^{-1}$) accounted for 74% of the total ±[^{3}H]-epibatidine binding and the low-affinity site (B_{max2}=11±4 fmol (mg protein)$^{-1}$) accounted for 26%. Thus, α4-containing rat brain nicotinic receptors display both high- and low-affinity ±[^{3}H]-epibatidine binding. Based on the two-site fit to the ±[^{3}H]-epibatidine concentration-binding data (Figure 3), 55% of the ±[^{3}H]-epibatidine binding sites should be occupied at a concentration of 30 pM, similar to the 40% occupancy predicted from the oocyte α4β2 kinetic data (above). The ±[^{3}H]-epibatidine bound to mAb-299-precipitated rat brain receptors (2 μg mAb 299 per well) incubated in a saturating (30 nM) ±[^{3}H]-epibatidine concentration was 30±3 fmol ±[^{3}H]-epibatidine (mg protein)$^{-1}$ (mean±s.e.mean, n=6). Correcting for the mAb 299 immunoprecipitation efficiency (see Methods), the density of mAb-299-precipitable ±[^{3}H]-epibatidine binding sites in the rat brain Triton X-100 extract should be 115±12 fmol ±[^{3}H]-epibatidine (mg protein)$^{-1}$. This value exceeds the previously measured B_{max} (80 fmol (mg protein)$^{-1}$) for ±[^{3}H]-epibatidine binding to rat forebrain homogenates (Houghtling *et al*., 1995) and the B_{max} (~50 fmol (mg protein)$^{-1}$) for −[^{3}H]-nicotine binding to non-detergent rat brain membrane extracts (Marks *et al*., 1986). However, previous results show that Triton X-100 (1%) extraction enriches the density of [^{3}H]-nicotine binding sites per mg of protein in rat brain extracts (Abood *et al*., 1980). Therefore, rat brain nicotinic receptors represent a greater fraction of the Triton X-100-soluble rat brain proteins than of the total rat brain proteins.

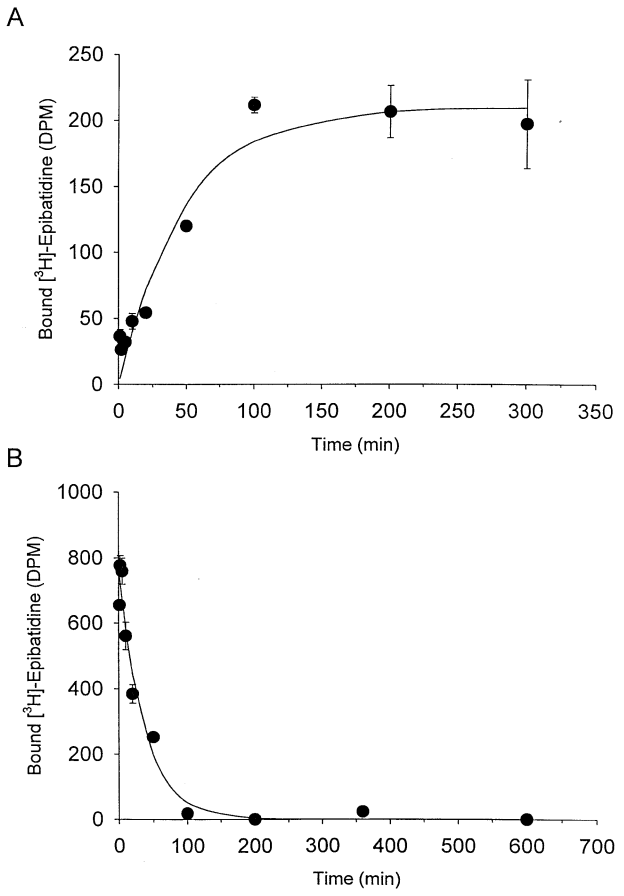

Figure 2 Time course of 30 pM ±[^{3}H]-epibatidine binding to (A) and dissociation from (B) mAb-299-precipitated rat α4β2 nicotinic receptors expressed in *Xenopus* oocytes. The error bars are ±s.e.mean (n=4 replicates). (A) The symbols denote the amount of ±[^{3}H]-epibatidine bound per well (in DPM) 1–300 min after the addition of 30 pM ±[^{3}H]-epibatidine. The line is a non-linear, least-squares fit to the equation:

$$B = B_\infty(1 - e^{-k_f t}), \quad (4)$$

where t is time after the addition of 30 pM ±[^{3}H]-epibatidine, B is amount of ±[^{3}H]-epibatidine bound at time t, B_∞ is the ±[^{3}H]-epibatidine bound at t=∞, and k_f is the apparent association rate constant for 30 pM ±[^{3}H]-epibatidine. B_∞=210±20 DPM (mean±s.e., d.f.=7). (B) The points denote the amount of bound ±[^{3}H]-epibatidine (in DPM) in the wells 1–600 min after a 4 h pre-incubation in 30 pM ±[^{3}H]-epibatidine, followed by the addition of 1 mM cold (−)nicotine at time zero. The line is a fit to:

$$B = B_0 e^{-k_b t}, \quad (5)$$

where t is the time after the addition of 1 mM (−)nicotine, B_0 is the ±[^{3}H]-epibatidine bound at time zero, and k_b is apparent dissociation rate constant. B_0=760±40 DPM (d.f.=8). See Results for the values of k_b and k_f.

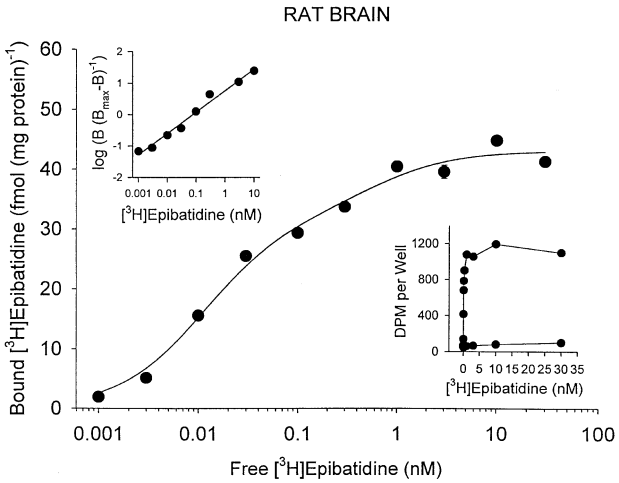

Figure 3 The ±[^{3}H]-epibatidine concentration-binding relation for mAb-299-precipitated rat brain receptors. The symbols are the amount of bound ±[^{3}H]-epibatidine (in fmol (mg protein)$^{-1}$). The error bars are ±s.e.mean but are obscured by the symbols in most cases (n=2 replicates). The line is a non-linear, least-squares fit to a two-binding site model,

$$B = \frac{B_{max1}}{1 + \frac{K_{D1}}{[epi]}} + \frac{B_{max2}}{1 + \frac{K_{D2}}{[epi]}}, \quad (6)$$

where B is the bound ±[^{3}H]-epibatidine, [epi] is the free ±[^{3}H]-epibatidine concentration, B_{max1} and B_{max2} are the maximum amounts of ±[^{3}H]-epibatidine bound to the high- and low-affinity receptor populations, and K_{D1} and K_{D2} are the apparent equilibrium dissociation constants for the high- and low-affinity receptors. See Results for the values of B_{max1}, B_{max2}, K_{D1} and K_{D2}. Upper left inset is a Hill plot of the ±[^{3}H]-epibatidine concentration-binding data. See Results for the slope (n_H) of regression line. B_{max} for the Hill transform was defined as the maximum observed ±[^{3}H]-epibatidine binding. The symbols in the lower right inset show the total and nonspecific bound ±[^{3}H]-epibatidine (in DPM per well). Line segments connect the symbols. The error bars are obscured by symbols.

Most mAb-299-precipitated rat brain receptors contain β2

The β4 subunit is present in the rat brain (Dineley-Miller & Patrick, 1992) and forms functional nicotinic receptors with α4 subunits in *Xenopus* oocytes (Duvoisin *et al*., 1989). However, it is far less abundant than the β2 subunit (Zoli *et al*., 1995). To determine what percentage of mAb-299-precipitated rat brain receptors contain β2, we measured the fraction of maximum ±[^{3}H]-epibatidine binding immunodepleted from rat brain extracts by serial pre-incubations with the anti-β2 antibody mAb 270 (see Methods). We used a saturating ±[^{3}H]-epibatidine concentration (30 nM) for these experiments. Three serial mAb 270 immunodepletions removed 97% of the mAb 270-precipitable ±[^{3}H]-epibatidine receptors from the rat brain extracts and 87% of the mAb-299-precipitable ±[^{3}H]-epibatidine receptors (Figure 4). Thus, 89% (87% $(0.97)^{-1}$) of the mAb-299-precipitated receptors in the rat brain contained β2.

±[^{3}H]-Epibatidine binding to heterologously expressed α4β2 receptors

Similar to the mAb-299-precipitated rat brain receptors (above), the Hill coefficients for ±[^{3}H]-epibatidine binding to the oocyte ($n_H = 0.69 \pm 0.03$, d.f. = 6) and adenoviral-expressed CV-1 α4β2 receptors (0.70 ± 0.02, d.f. = 2) were less than unity. Therefore, we fit the ±[^{3}H]-epibatidine concentration-binding data for the oocytes (Figure 5) and adenoviral-infected CV-1 cells (Figure 6A) to a two-site model. The K_Ds for ±[^{3}H]-epibatidine binding to the oocyte α4β2 receptors were 14 ± 2 pM and 1.2 ± 0.5 nM (d.f. = 8). Likewise, the K_Ds for ±[^{3}H]-epibatidine binding to the adenoviral-infected CV-1 α4β2 receptors were 7 ± 2 pM and 1 ± 2 nM (d.f. = 6). These K_Ds were not significantly different from those of the native brain receptors (11 ± 4 pM, 560 ± 70 pM). Moreover, the high-affinity oocyte site accounted for nearly the same percentage (73%) to total ±[^{3}H]-epibatidine binding sites as the high-affinity site of native brain receptors did (74%). The high-affinity sites in the adenoviral-infected CV-1 cells accounted for a somewhat higher percentage (85%) of the total binding sites. The oocyte equilibrium binding data predicted 50% receptor occupancy in 30 pM ±[^{3}H]-epibatidine, similar to the 40% occupancy rate predicted from the kinetic data (Figure 1A,B). The Hill coefficient (1.0 ± 0.2, d.f. = 7) for ±[^{3}H]-epibatidine binding to rat α4β2 receptors expressed in CV-1 cells with vaccinia virus was larger than that for the other expression systems, suggesting a more homogenous receptor population. Therefore, we fitted the vaccinia viral ±[^{3}H]-epibatidine concentration-binding data to a single binding site model. The resulting K_D (40 ± 3 pM, d.f. = 8) was somewhat larger than the high-affinity K_D for native brain receptors (11 ± 4 pM) and α4β2 receptors expressed in oocytes (14 ± 2 pM). This discrepancy could be due to an unresolved population of low-affinity ±[^{3}H]-epibatidine binding sites in the vaccinia infected-transfected cells.

Native and heterologously expressed receptors have similar DHβE and NDNI K_i*s*

To compare the antagonist profiles of the native brain and heterogously expressed α4β2 receptors, we measured the effects of two competitive antagonists (DHβE, NDNI) on 30 pM ±[^{3}H]-epibatidine binding to these receptors (Figures 7–8, Table 1). Figure 8A shows the structure of the novel antagonist NDNI. At a concentration of 30 pM ±[^{3}H]-epibatidine, we were primarily measuring antagonism of the high-affinity ±[^{3}H]-epibatidine binding sites because the fractional occupancy of the low-affinity sites was only 3–5% at this ±[^{3}H]-epibatidine concentration (assuming a low-affinity K_D of 0.6–1 nM). DHβE was a more potent antagonist ($IC_{50} = 260$–470 nM) than NDNI ($IC_{50} = 7$–10 μM) (Table 1) and inhibited ±[^{3}H]-epibatidine binding to the high-affinity site ~ten times more potently than NDNI. The native brain and heterologously expressed α4β2 receptors displayed no significant differences in regard to DHβE (Figure 7) and NDNI (Figure

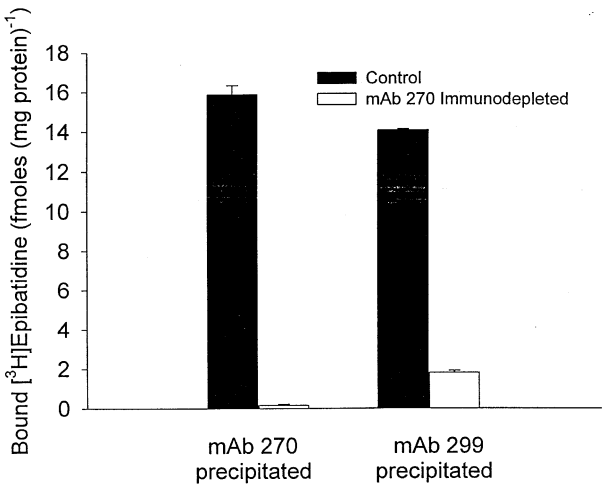

Figure 4 Three overnight mAb 270 pre-incubations depleted most of the mAb-270- and mAb-299-precipitable ±[^{3}H]-epibatidine binding from the rat brain extracts. The free ±[^{3}H]-epibatidine concentration was 30 nM. Control extracts were pre-incubated three times with sepharose beads without antibody. MAb-270-immunodepleted extracts were pre-incubated three times with mAb 270 and sepharose beads. See Methods for additional procedural details. Error bars are ±s.e.mean ($n = 5$ replicates).

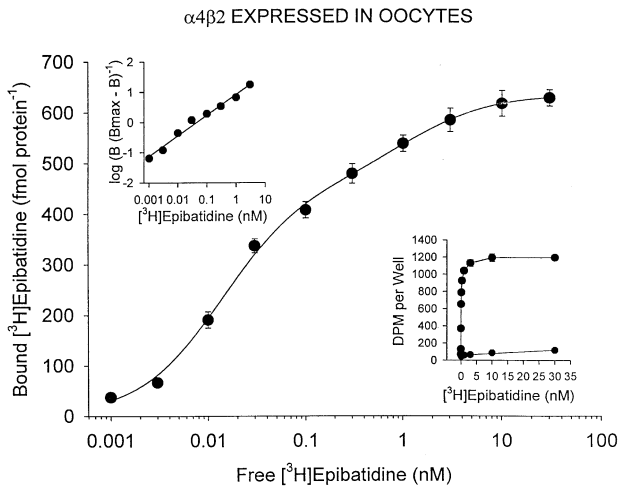

Figure 5 The ±[^{3}H]-epibatidine concentration-binding relation for mAb-299-precipitated rat α4β2 nicotinic receptors expressed in *Xenopus* oocytes. The symbols are the amount of bound ±[^{3}H]-epibatidine (in fmol (mg protein)$^{-1}$). The error bars are ±s.e.mean ($n = 2$ replicates). The line is a non-linear, least squares fit to a two-binding site model. B_{max1} (high-affinity binding) = 460 ± 20 fmol (mg protein)$^{-1}$. B_{max2} (low-affinity binding) = 170 ± 20 fmol (mg protein)$^{-1}$. See Results for the values of the K_Ds. The upper and lower insets are similar to those in Figure 3.

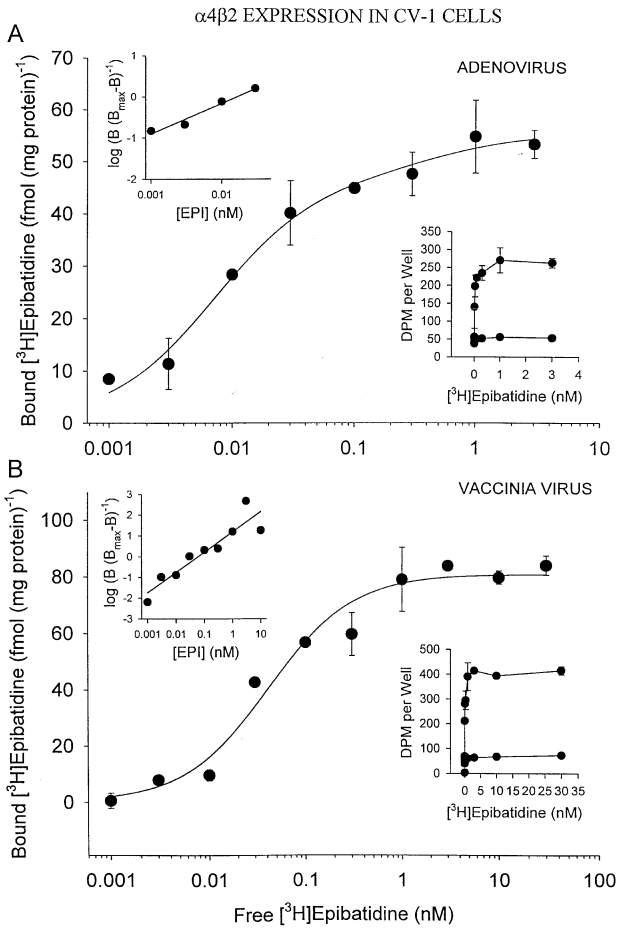

Figure 6 $\pm$[^{3}H]-epibatidine concentration-binding relations for mAb-299-precipitated rat $\alpha4\beta2$ receptors expressed in CV-1 cells using recombinant adenovirus (A) or vaccinia viral infection/transfection (B) (see Methods for procedural details). (A) The line is a non-linear, least-squares fit to a two-binding site model. $B_{max1} = 47 \pm 3$ fmol (mg protein)$^{-1}$ (high-affinity site). $B_{max2} = 8 \pm 5$ fmol (mg protein)$^{-1}$. See Results for the K_Ds. (B) The line is a non-linear, least squares fit to a single binding site model,

$$B = \frac{B_{max}}{1 + \frac{K_D}{[epi]}} \quad (7)$$

$B_{max} = 80 \pm 3$ fmol (mg protein)$^{-1}$. The insets are similar to those in Figures 3 and 5. The error bars are $\pm$s.e.mean ($n = 2$ replicates).

8B) inhibition of $\pm$[^{3}H]-epibatidine binding (Table 1). However, the DHβE K_is for the native and heterologously expressed receptors (50–130 nM, Table 1) were somewhat larger than that predicted (16 nM) from the inhibition of $\pm$[^{3}H]-epibatidine binding to rat forebrain homogenates by DHβE (Houghtling *et al*., 1995).

Discussion

Our results show that rat $\alpha4\beta2$ nicotinic receptors expressed in *Xenopus* occytes or CV-1 cells and, native rat brain nicotinic receptors containing $\alpha4$ and $\beta2$ subunits, display similar pharmacological properties in regard to $\pm$[^{3}H]-epibatidine binding and the inhibition of high-affinity $\pm$[^{3}H]-epibatidine binding by the competitive antagonists DHβE and NDNI. Similar to previous studies of rat brain nicotinic receptors (Whiting & Lindstrom, 1987; Flores *et al*., 1991), our

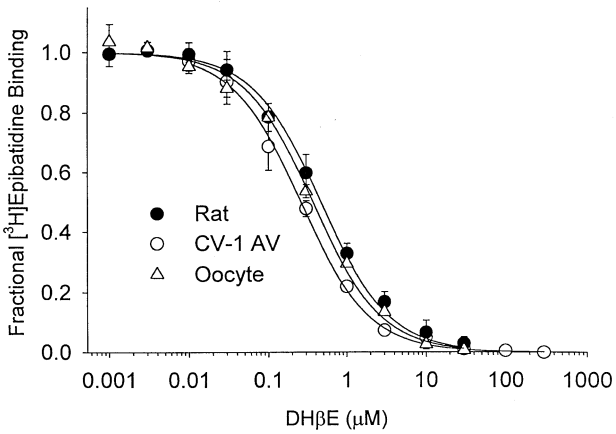

Figure 7 DHβE inhibited 30 pM $\pm$[^{3}H]-epibatidine binding to mAb-299-precipitated rat brain receptors (Rat), rat $\alpha4\beta2$ receptors expressed in oocytes (Oocyte), and rat $\alpha4\beta2$ receptors expressed in CV-1 cells with recombinant adenovirus (CV-1 AV) equally well. The symbols denote the mean fractional $\pm$[^{3}H]-epibatidine binding at various DHβE concentrations. The lines are non-linear, least squares fits to equation 1 (see Methods). See Table 1 for the DHβE IC_{50}s and K_is. The error bars are $\pm$s.e.mean ($n = 4$ for rat brain; $n = 2$ for $\alpha4\beta2$ receptors expressed in oocytes and CV-1 cells with adenovirus).

Table 1 IC_{50}s and k_is for the competitive antagonists

Receptor	*Host cell*	*Inhibitor*	*IC_{50}** (μM)	*High-affinity $\pm$[^{3}H]-Epibaditine* K_d* (pM)	K_i^+ (μM)
Rat brain	neurons	DHβE	0.47$\pm$0.03 (10)	20$\pm$10 (8)	0.2$\pm$0.1
		NDNI	9$\pm$1 (10)		4$\pm$3
Rat $\alpha4\beta2$	oocytes	DHβE	0.37$\pm$0.02 (10)	30$\pm$6 (8)	0.2$\pm$0.1
		NDNI	7$\pm$1 (10)		4$\pm$2
Rat $\alpha4\beta2$	CV-1 AV#	DHβE	0.26$\pm$0.01 (10)	8$\pm$2 (6)	0.05$\pm$0.02
		NDNI	10$\pm$1 (10)		2$\pm$1

*$\pm$s.e. (degrees of freedom); $^+$ $\pm$ s.e.; #CV-1 cells using adenoviral infection; The $\pm$[^{3}H]-epibatidine concentration in the inhibitor experiments was 30 pM.

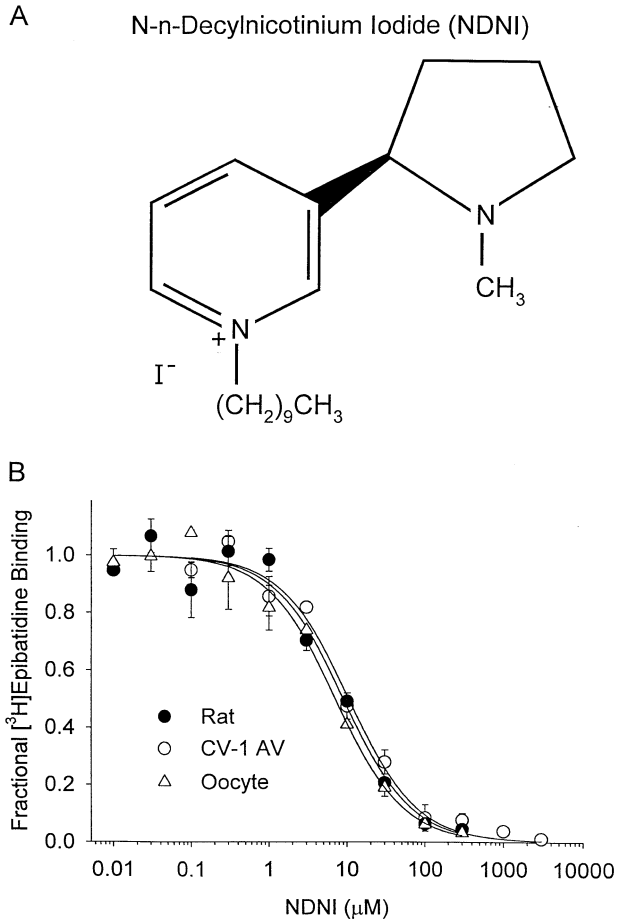

Figure 8 (A) Structural formula of N-n-decylnicotinium iodide (NDNI). (B) NDNI inhibited 30 pM $\pm$[^{3}H]-epibatidine binding to mAb-299-precipitated rat brain, rat $\alpha4\beta2$ receptors expressed in oocytes, and rat $\alpha4\beta2$ receptors expressed in CV-1 cells (using adenovirus) equally well. The lines are fits to equation 1 (see Methods). See Table 1 for the NDNI IC_{50}s and K_is. The error bars are $\pm$s.e.mean ($n=2$ replicates).

immunodepletion experiments further show that most $\alpha4$-containing nicotinic receptors in the rat brain also contain $\beta2$. Moreover, $\alpha4\beta2$ receptors expressed in native brain neurons, oocytes, and CV-1 cells with adenovirus all exhibit both high- and low-affinity $\pm$[^{3}H]-epibatidine binding. Previous studies of chick brain nicotinic receptors immunoprecipitated with mAb 299 show that the pharmacological properties and macromolecular size of these receptors also resemble those of heterologously expressed chick $\alpha4\beta2$ nicotinic receptors immunoprecipitated with the anti-$\beta2$ antibody mAb 290 (Whiting *et al*., 1991).

Nicotinic receptors in rat forebrain homogenates display both high- ($K_D=15$ pM) and low affinity ($K_D=360$ pM) $\pm$[^{3}H]-epibatidine binding (Houghtling *et al*., 1995). Our experiments show that $\alpha4$ subunits are present in both types of binding sites. MAb 270 immunodepletion experiments further show that 89% of the mAb-299-precipitated binding sites contain $\beta2$. Since the high-affinity sites account for only 74% of the total mAb-299-precipitated rat brain $\pm$[^{3}H]-epibatidine binding sites, at least some low-affinity rat brain receptors ($\geqslant58\%$) must contain both $\alpha4$ and $\beta2$ subunits. In support of this hypothesis, we find that $\alpha4\beta2$ receptors expressed in *Xenopus* oocytes and CV-1 cells display both low- and high-affinity $\pm$[^{3}H]-epibatidine binding.

Comparisons between the properties of native and recombinant ganglionic nicotinic receptors (Sivilotti *et al*., 1997; Lewis *et al*., 1997) suggest that the host cell can affect the biophysical properties of ganglionic nicotinic receptors. The relative sensitivity of rat nicotinic receptors in the rat superior cervical ganglion (SCG) to different nicotonic agonists (except DMPP) resembles that of rat $\alpha3\beta4$ receptors expressed in *Xenopus* oocytes (Covernton *et al*., 1994). However, the single-channel conductance and burst duration of the native rat SCG receptors are significantly different (Lewis *et al*., 1997; Sivilotti *et al*., 1997). In contrast, mouse fibroblasts expressing rat $\alpha3\beta4$ receptors contain one population of nicotinic channels with properties resembling those of the native SCG nicotinic receptor and another with properties resembling those of the rat $\alpha3\beta4$ receptors expressed in *Xenopus* oocytes (Lewis *et al*., 1997; Sivilotti *et al*., 1997). Thus, mammalian cell lines, but not *Xenopus* oocytes, appear to be capable of assembling a population of $\alpha3\beta4$ channels with single-channel properties similar to the native ones.

The host cell type appears to affect the properties of brain nicotinic receptors less than those of ganglionic nicotinic receptors. The conductance (49 pS) of rat $\alpha4\beta2$ channels expressed in oocytes closely matches that of human $\alpha4\beta2$ channels (46 pS) expressed in HEK 293 cells (Buisson *et al*., 1996; Figl *et al*., 1998). Moreover, the EC_{50} and Hill coefficient of rat and human $\alpha4\beta2$ ACh concentration-response relations are nearly identical (Buisson *et al*., 1996; Figl *et al*., 1998). Our results show that $\alpha4\beta2$ nicotinic receptors immunoprecipitated from rat brain neurons, *Xenopus* oocytes, and CV-1 cells display similar pharmacological properties in regard to $\pm$[^{3}H]-epibatidine binding and the competitive inhibition of $\pm$[^{3}H]-epibatidine binding by DHβE and NDNI. Thus, *Xenopus* oocytes appear to be capable of synthesizing an $\alpha4\beta2$ receptor with pharmacological properties similar to those expressed in rat neurons and mammalian cell lines despite differences in the receptor assembly and synthesis temperature (18°C versus 36 °C) and potential differences in folding proteins.

Heterologous expression provides the only available means of studying the pharmacological and biophysical properties of identified neuronal nicotinic receptor subtypes. The relevance of the results for heterologously expressed receptors depends on how closely the properties of those receptors match the properties of the native receptors. Our results show that rat $\alpha4\beta2$ nicotinic receptors expressed in *Xenopus* oocytes and CV-1 cells display similar pharmacological behaviour in regard to at least three drugs, $\pm$[^{3}H]-epibatidine, DHβE, and NDNI. Further research using this approach will tell us if these similarities extend to other types of competitive antagonists.

We thank Dr Kenneth Dorshkind of the University of California, Los Angeles (Los Angeles, U.S.A.) for providing mAb 270 ascites. This research was supported by grants from the American Heart Association, California Affiliate (#96–254), the UC Tobacco-related Disease Program (TRDRP), and the NIH (#RO1DA10934).

References

ABOOD, L.G., REYNOLDS, D.T. & BIDLACK, J.M. (1980). Stereospecific ^{3}H-nicotine binding to intact and solubilized rat brain membranes and evidence for its noncholinergic nature. *Life Sciences,* **27,** 1307 – 1314.

BUISSON, B., GOPALAKRISHNAN, M., ARNERIC, S.P., SULLIVAN, J.P. & BERTRAND, D. (1996). Human $\alpha 4\beta 2$ neuronal nicotinic acetylcholine receptor in HEK 293 cells: a patch clamp study. *J. Neurosci.,* **16,** 7880 – 7891.

COOPER, E., COUTURIER, S. & BALLIVET, M. (1991). Pentameric structure and subunit stoichiometry of a neuronal nicotinic acetylcholine receptor. *Nature,* **350,** 235 – 238.

COVERNTON, P.J.O., KOJIMA, H., SIVILOTTI, L.G., GIBB, A.J. & COLQUHOUN, D. (1994). Comparison of neuronal nicotinic receptors in rat sympathetic neurones with subunit pairs expressed in *Xenopus* oocytes. *J. Physiol.,* **481,** 27 – 34.

CROOKS, P.A., RAVARD, A., WILKINS, L.M., PENG, L.-H., BUXTON, S.T. & DWOSKIN, L.P. (1995). Inhibition of nicotine-evoked [^{3}H]dopamine release by pyridine n-substituted analogues: a new class of nicotinic antagonist. *Drug Develop. Res.,* **36,** 91 – 102.

DINELY-MILLER, K. & PATRICK, J. (1992). Gene transcripts for the nicotinic acetylcholine receptor subunit, Beta 4, are distributed in multiple areas of the rat central nervous system. *Mol. Brain. Res.,* **16,** 339 – 344.

DUVOISIN, R.M., DENERIS, E.S., PATRICK, J. & HEINEMANN, S. (1989). The functional diversity of the neuronal nicotinic acetylcholine receptors is increased by a novel subunit: $\beta 4$. *Neuron.,* **3,** 487 – 496.

ELROY-STEIN, O., FUERST, T.R. & MOSS, B. (1989). Cap-independent translation of mRNA conferred by encephalomyocarditis virus 5′ sequence improves the performance of the vaccinia virus/bacteriophage T7 hybrid expression system. *Proc. Nat. Acad. Sci. U.S.A.,* **86,** 6126 – 6130.

FIGL, A., VISESHAKUL, N., SHAFAEE, N., FORSAYETH, J. & COHEN, B.N. (1998). Two mutations linked to nocturnal frontal lobe epilepsy cause use-dependent potentiation of the nicotinic ACh response. *J. Physiol.,* **513.3,** 655 – 670.

FLORES, C.M., ROGERS, S.W., PABREZA, L.A., WOLFE, B.B. & KELLAR, K.J. (1991). A subtype of nicotinic cholinergic receptor in rat brain is composed of $\alpha 4$ and $\beta 4$ subunits and is up-regulated by chronic nicotine treatment. *Mol. Pharmacol.,* **41,** 31 – 37.

FUERST, T.R., NILES, E.G., STUDIER, F.W. & MOSS, B. (1986). Eukaryotic transient expression system based on recombinant vaccinia virus that synthesizes bacteriophage T7 RNA polymerase. *Proc. Natl. Acad. Sci. U.S.A.,* **83,** 8122 – 8126.

GERZANICH, V., PENG, X., WANG, F., WELLS, G., ANAND, R., FLETCHER, S. & LINDSTROM, J. (1995). Comparative pharmacology of epibatidine: a potent agonist for neuronal nicotinic acetylcholine receptors. *Mol. Pharmacol.,* **48,** 774 – 782.

GOSSEN, M. & BUJARD, H. (1992). Tight control of gene expression in mammalian cells by tetracycline responsive promoters. *Proc. Natl. Acad. Sci. U.S.A.,* **89,** 5547 – 5551.

HARDY, S., KITAMURA, M., HARRIS-STANSIL, T., DAI, Y. & PHIPPS, M.L. (1997). Construction of adenovirus vectors through Cre-lox recombination. *J. Virol.,* **71,** 1842 – 1849.

HILL, J.A., ZOLI, M., BOURGEOIS, J.-P. & CHANGEUX, J.-P. (1993). Immunocytochemical localization of a neuronal nicotinic receptor: the $\beta 2$ subunit. *J. Neurosci.,* **13,** 1551 – 1568.

HOUGHTLING, R.A., DAVILA-GARCIA, M.I. & KELLAR, K.J. (1995). Characterization of $(\pm)$-[^{3}H]epibatidine binding to nicotinic cholinergic receptors in rat and human brain. *Mol. Pharmacol.,* **48,** 280 – 287.

JONES, N. & SHENK, T. (1979). Isolation of adenovirus type 5 host range deletion mutants defective for transformation of rat embryo cells. *Cell,* **17,** 683 – 689.

LEWIS, T.M., HARKNESS, P.C., SIVILOTTI, L.G., COLQUHOUN, D. & MILLER, N.S. (1997). The ion channel properties of a rat recombinant neuronal nicotinic receptor are dependent on host cell type. *J. Physiol.,* **502,** 299 – 306.

MARKS, M.J., STITZEL, J.A., ROMM, E., WEHNER, J.M. & COLLINS, A.C. (1986). Nicotinic binding sites in rat and mouse brain: comparison of acetylcholine, nicotine, and α-bungarotoxin. *Mol. Pharmacol.,* **30,** 427 – 436.

MARKS, M.J., WHITEAKER, P., CALCATERRA, J., STITZEL, J.A., BULLOCK, A., GRADY, S.R., PICCIOTTO, M.R., CHANGEUX, J.-P. & COLLINS, A.C. (1999). Two pharmacologically distinct components of nicotinic receptor-mediated rubidium efflux in mouse brain require the $\beta 2$ subunit. *J. Pharm. & Exp. Therap.,* **289,** 1090 – 1103.

MARUBIO, L.M., ARROYO-JIMENEZ, M.D.M., CORDERO-ERAUSQUIN, M., LENA, C., LE NOVERE, N., DE KERCHOVE D'EXAERDE, A., HUCHET, M., DAMAJ, M.I. & CHANGEUX, J.-P. (1999). Reduced antinoiception in mice lacking neuronal nicotinic receptor subunits. *Nature,* **398,** 805 – 810.

MOOD, A.M., GRAYBILL, F.A. & BOES, D.C. (1974). Introduction to the theory of statistics. New York: McGraw-Hill Company, pp. 180 – 181.

NEERING, S.J., HARDY, S.F., MINAMOTO, D., SPRATT, S.K. & JORDAN, C.T. (1996). Transduction of primative human hematopoietic cells with recombinant adenovirus vectors. *Blood,* **88,** 1147 – 1155.

PENG, X., GERZANICH, V., ANAND, R., WHITING, P.J. & LINDSTROM, J. (1994). Nicotine-induced increase in neuronal nicotinic receptors results from a decrease in the rate of receptor turnover. *Mol. Pharmacol.,* **46,** 523 – 530.

PICCIOTTO, M.R., ZOLI, M., LENA, C., BESSIS, A., LALLEMAND, Y., LE NOVERE, N., VINCENT, P., PICH, E.M., BRULET, P. & CHANGEUX, J.-P. (1995). Abnormal avoidance learning in mice lacking functional high-affinity nicotine receptor in brain. *Nature,* **374,** 65 – 67.

QUICK, M.W. & LESTER, H.A. (1994). Methods for expression of excitability proteins in *Xenopus* oocytes. *Meth. Neurosci.,* **19,** 261 – 279.

SARGENT, P.B. (1993). The diversity of neuronal nicotinic acetylcholine receptors. *Ann. Rev. Neurosci.,* **16,** 403 – 443.

SIVILOTTI, L.G., MCNEIL, D.K., LEWIS, T.M., NASSAR, M.A., SCHOEPFER, R. & COLQUHOUN, D. (1997). Recombinant nicotinic receptors, expressed in *Xenopus* oocytes, do not resemble native rat sympathetic ganglion receptors in single-channel behaviour. *J. Physiol.,* **500,** 123 – 138.

WHITING, P. & LINDSTROM, J. (1986). Pharmacological properties of immuno-isolated neuronal nicotinic receptors. *J. Neurosci.,* **6,** 3061 – 3069.

WHITING, P. & LINDSTROM, J. (1987). Purification and characterization of a nicotinic acetylcholine receptor from rat brain. *Proc. Natl. Acad. Sci. U.S.A.,* **84,** 595 – 599.

WHITING, P. & LINDSTROM, J. (1988). Characterization of bovine and human neuronal nicotinic acetylcholine receptors using monoclonal antibodies. *J. Neurosci.,* **8,** 3395 – 3404.

WHITING, P., SCHOEPFER, R., LINDSTROM, J. & PRIESTLEY, T. (1991). Structural and pharmacological characterization of the major brain nicotinic acetylcholine receptor subtype stably expressed in mouse fibroblasts. *Mol. Pharmacol.,* **40,** 463 – 472.

ZOLI, M., LE NOVERE, N., HILL, J.A. JR. & CHANGEUX, J.-P. (1995). Developmental regulation of nicotinic ACh receptor subunit mRNAs in the rat central and peripheral nervous systems. *J. Neurosci.,* **15,** 1912 – 1939.

ZOLI, M., LENA, C., PICCIOTTO, M.R. & CHANGEUX, J.-P. (1998). Identification of four classes of brain nicotinic receptors using $\beta 2$ mutant mice. *J. Neurosci.,* **18,** 4461 – 4472.

(Received July 26, 1999
Revised August 12, 1999
Accepted August 26, 1999)